Separation of radiation and absorption losses in two-dimensional photonic crystal single defect cavities

I. Alvarado-Rodriguez[a] and E. Yablonovitch
Department of Electrical Engineering, University of California, Los Angeles, California 90095

(Received 24 June 2002; accepted 3 September 2002)

We have characterized the optical modes present in a two-dimensional photonic crystal single defect cavity fabricated in an InP/$In_{0.53}Ga_{0.47}As$/InP double heterostructure thin film on a glass slide. The cavity resonance was tuned to different frequencies in the 1.55 μm spectral region. Radiation losses and material absorption influence the measured value of cavity quality factor Q. We separated these two loss mechanisms by performing a curve fit of the loss rate $1/Q$ versus the wavelength-dependent absorption coefficient of $In_{0.53}Ga_{0.47}As$. By extrapolating this curve to zero absorption, the radiation loss rate $1/Q_{rad}$ is obtained. © *2002 American Institute of Physics.* [DOI: 10.1063/1.1516835]
42.70.QS, 42.82.m

I. INTRODUCTION

Recently, there has been interest in optical cavities and other devices based on two-dimensional (2D) photonic crystal slabs.[1–12] The diverse potential functions of 2D photonic crystals have made them attractive for optical integration. Furthermore, the fabrication process of 2D photonic crystals is compatible with the well-developed planar fabrication technology used in electronic integrated circuits. In particular, 2D photonic crystals are interesting due to the potential of achieving a high-cavity Q. Theoretical and experimental work on how to design a high-Q cavity has been reported.[1–12] A significant amount of research has been concentrated on devices on 2D photonic crystals based on free-standing membranes as well as on a transparent substrate. In our work, we have placed our devices on a a glass slide, which is better in terms of device robustness and fabrication yield at the expense of reducing the optical confinement of the device.

The characterization of 2D photonic crystals has been made mostly by measuring the spectrum of photoluminescence[4,5,13] and electroluminescence.[14] These techniques are useful and relatively easy to perform due to the fact that the light is generated inside the cavity. In this way, the coupling of the light into the optical cavity is very strong and the cavity signature is clearly evident in the emitted photoluminescence spectrum. However, the fact that the material is capable of producing light means that it can also absorb light. Loss due to material absorption reduces optical confinement in the cavity. In order to reduce the material absorption, some research groups have made and characterized 2D photonic crystal-based devices on semiconductor substrates with quantum dots[4,5] rather than quantum wells. However, these devices have been designed to operate at wavelengths below 1.3 μm.

In this article, we present results on fabrication and characterization of 2D photonic crystal cavities based on an electromagnetic mode that is induced when a defect in the photonic crystal is created. In Sec. II, the device design and fabrication process is described. This process is based on dry etching in semiconductors followed by removal of the growth substrate by selective wet etching. In Sec. III, the characterization results are presented. The cavities are characterized by measuring the photoluminescence spectrum. By modifying the lattice period, the cavity resonance wavelength was tuned to the 1.55-μm spectral region. The measured cavity Q is limited by a combination of radiation losses and material absorption losses. By taking into account the material absorption as a function of the wavelength, we are able to determine the radiation loss limited cavity Q.

II. CAVITY DESIGN AND FABRICATION

We make 2D photonic crystals in a thin epitaxial semiconductor layer by drilling holes arranged in a triangular lattice. After removal of the growth substrate by selective etching, the thin layer is transferred onto a glass slide. The absence of a hole at the center of the photonic crystal forms a defect state in the photonic band gap, which in this case is an optical cavity. The sample layout is shown in Fig. 1(a).

The cavities are fabricated on InP/$In_{0.53}Ga_{0.47}As$/InP double heterostructure semiconductor material; the thickness of each layer is 90/60/90 nm respectively. The layers were grown by metal-organic chemical vapor deposition on an InP substrate. An intermediate 1.5-mm InGaAs layer was grown in between the InP substrate and the double hetersotructure. This layer serves as a stopetch for substrate removal. On the epilayer, we deposit a 200-nm thick layer of SiO2 by plasma-enhanced chemical vapor deposition, and then coat the sample with 200 nm of polymethylmethacrylate (PMMA). A triangular array of holes is defined in the PMMA layer by electron-beam lithography using Leica EBL100. The pattern is transferred to the SiO2 film and to the semiconductor heterostructure by CHF3 based reactive ion etching (RIE) and Cl+Ar chemically assisted ion-beam etching. The use of CHF3 RIE simplifies the fabrication process since it allows a more effective pattern transfer from the PMMA to the SiO2 film.[15] This is the standard fabrication technique for these

[a]Electronic address: ialva@ee.ucla.edu

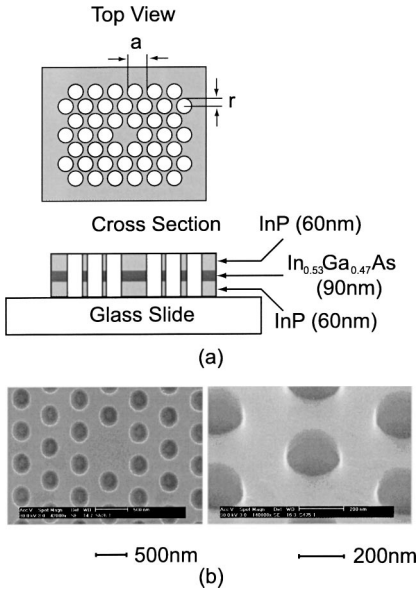

FIG. 1. Sample layout, where a is the lattice parameter and r is the hole radius. The patterned film is pasted onto a glass substrate. (b) Scanning electron micrographs of the fabricated device.

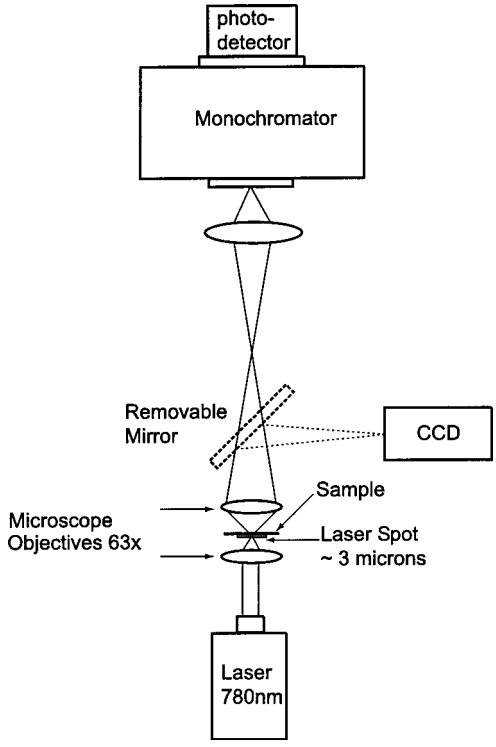

FIG. 2. Experimental setup. The 780-nm pump laser is focused on the semiconductor film side of the sample and the resulting photoluminescence signal is collected from the glass side.

structures, which has been developed and used for several years now.[16–18] After patterning and etching, the specimen is attached upside down on a glass slide using Norland 70 cement and the substrate is removed by selective wet etching. HCl is used to remove the InP substrate and $H_2SO_4:H_2O_2:H_2O$ is used to remove the intermediate InGaAs stopetch. By this method, we are able to effectively transfer the patterned thin film on a glass slide.

To tune the resonance frequency of the cavity, we fabricated devices with different lattice parameters (457, 500, and 525 nm), while preserving in all of them a void-filling factor of 35%. The overall size of the PC is around $60\,\mu$m $\times 40\,\mu$m. The fabricated PC cavity is shown in Fig 1(b).

III. CAVITY CHARACTERIZATION

Photoluminescence (PL) is induced by focusing the light of an AlGaAs laser diode (780 nm) onto the semiconductor coated side of the glass substrate. The laser beam is focused down to a spot of $\approx 3\,\mu$m in diameter. The light is then collected from the back side of the sample (the glass side) and sent through a spectrometer. The experimental setup is shown in Fig. 2. Two kinds of photodetectors were used to measure the spectrum: A conventional InGaAs p–n heterojunction at room temperature and a liquid N_2 cooled Ge detector. The latter detector to extend the optical bandwidth relative to the InGaAs detector.

We induced PL on three different points of the sample: The cavity portion of the photonic crystal, the periodic portion of the photonic crystal, and the unpatterned region of the sample. Figs. 3(a), 3(b), and 3(c) show the photoluminescence spectrum measured from these three points. The cavity spectral signature is evident in the collected photoluminescence spectrum and that sharp feature is spatially confined to the region near the cavity. Notice in Fig. 3 that the photoluminescence produced in the unpatterned region is significantly larger than that produced in the photonic crystal. This is due to several factors: There is less active material in the photonic crystal, the photoluminescence emission is partially inhibited since it lies within the band gap of the photonic crystal, and the quantum efficiency is reduced due to the presence of edges and the occurrence of surface recombination. By moving the pump-laser spot away from the cavity, the signal corresponding to the cavity decreases. The sharp cavity spectral feature totally vanishes when the pump-laser spot is about 4 μm away from the cavity. This is an indication of the spatial confinement of the optical mode.

As mentioned above, the cavity resonant wavelength was tuned by fabricating structures with different lattice parameters, as shown in Fig. 4. In this figure, the cavity resonance wavelengths are 1480, 1540, and 1610 nm, which correspond to structures with lattice parameters of 475, 500, and 525 nm, respectively. All these structures have roughly the same value of the resonance wavelength-lattice parameter ratio (λ_o/a), which is roughly 0.316. This value agrees with the design parameter obtained from numerical calculations.[19]

From Fig. 4, the cavity Q. can be calculated as $Q = \lambda_o/\Delta\lambda$, where $\Delta\lambda$ is the full width at half maximum of each peak. The value of Q corresponding to each structure is indicated on the same figure. As evidenced in Fig. 4, the value of the cavity Q decreases as the resonance wavelength decreases. Now, there are present in the structure two mechanisms of loss, namely, the material absorption and the radiation losses. Both mechanisms are present in the measured value of Q. In order to separate the different loss contributions, we recall the definition of the cavity Q value given by[20]

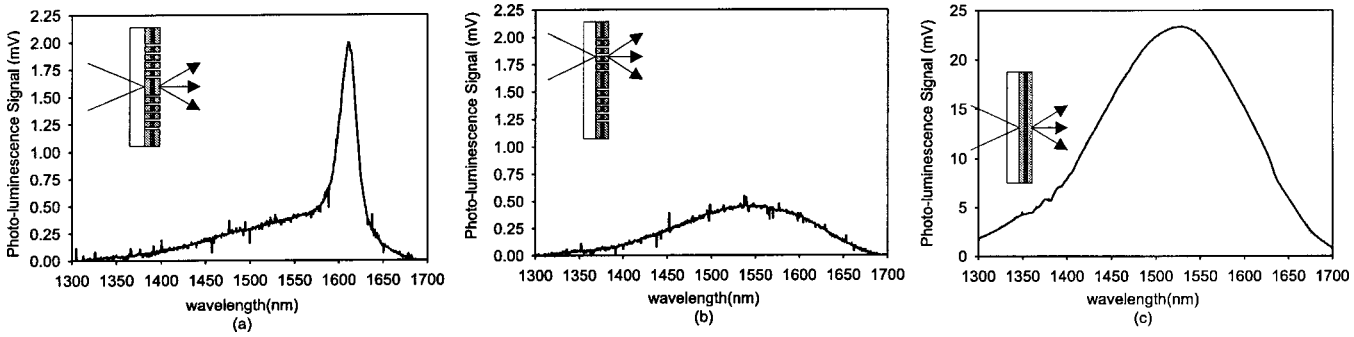

FIG. 3. Photoluminescence spectra obtained when the pump laser is focused on (a) the cavity region in the photonic crystal, (b) the defect-free photonic crystal, and (c) the unpatterned region of the sample. In particular, (b) was measured with the pump laser focused 4 μm away from the cavity. In this case, the lattice parameter of the structure was $a=525$ nm and the void-filling factor was 35%.

$$Q=\frac{\omega_o U}{W_L}, \tag{1}$$

where ω_o is the cavity resonance frequency, U is the energy stored in the mode, and W_L is the energy loss rate. The total loss rate is the sum of the material absorption rate and the radiation losses, thus we can rewrite Eq. (1) as

$$\frac{1}{Q}=\frac{W_L}{\omega_o U}=\frac{W_{\text{rad}}}{\omega_o U}+\frac{W_{\text{abs}}}{\omega_o U}=\frac{1}{Q_{\text{rad}}}+\frac{1}{Q_{\text{abs}}}, \tag{2}$$

where Q_{rad} and Q_{abs} account for the radiation loss and absorption, respectively. In Fig. 5, we plot the value $1/Q$ versus the absorption coefficient corresponding to each resonance wavelength. The absorption coefficient as a function of the wavelength for $In_{0.53}Ga_{0.47}As$ was obtained from Ref. 21. From Eq. (2), the dependence of the cavity Q and the absorption coefficient can be modelled as

$$\frac{1}{Q}=\frac{1}{Q_{\text{rad}}}+C\alpha(\lambda) \tag{3}$$

Where $a(\lambda)$ is the absorption coefficient, C is a proportionality constant, and Q_{rad} is the quality factor taking into account radiation losses only (structure exhibiting zero absorption). From the linear extrapolation to the case of zero absorption, we find that $Q_{\text{rad}}=320$. This value of Q_{rad} agrees well with theoretical calculations.[8,19] Higher-Q values have been recently reported for more sophisticated designs, using quantum dot luminescent semiconductors that have very low average absorption coefficients.

IV. CONCLUSIONS

We have fabricated and characterized 2D photonic crystal defect cavities based on perforated thin films on glass slides. The cavity characterization was performed by measuring the photoluminescence spectrum. The center wavelength can be tuned over the band used in optical telecommunications. The measured cavity Q is limited by the material absorption. A simple model is presented relating cavity Q to material absorption, and extrapolation to zero absorption is obtained. Further experimental and theoretical work is still required in order to obtain an optical cavity based on a 2D photonic crystal that exhibits a Q high enough to filter telecommunications channels.

ACKNOWLEDGMENTS

The authors thank H. Mossallaei for his help in numerical computation. This work was supported by DARPA CHIPS MDA972-00-1-0019. I.A.R. acknowledges support from the UC-MEXUS-CONACyT program.

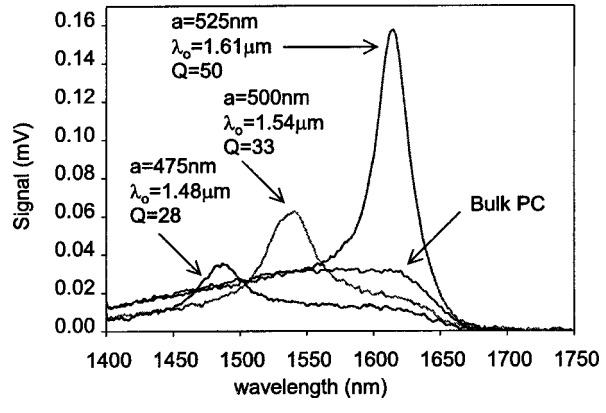

FIG. 4. Photoluminescence spectra from cavities for different photonic crystal-lattice parameters. The photoluminescence from the bulk photonic crystal is shown as a reference. All the structures have the same void-filling fraction of 35%. The signal fall off at 1650 nm is due to the optical limit of the InGaAs photodetector.

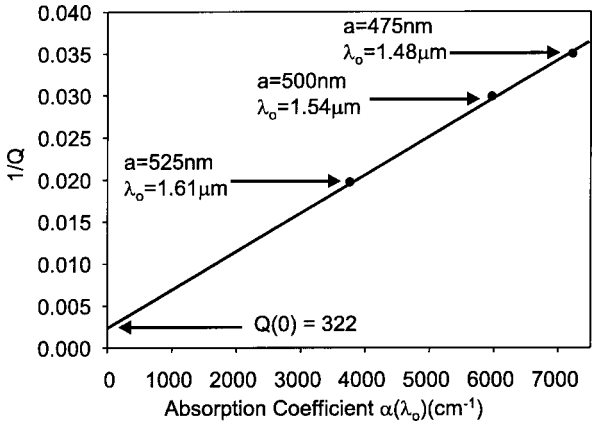

FIG. 5. Cavity quality factor $1/Q$ absorption obtained from the data of Fig. 4. The lattice parameter is a and λ_o is the cavity resonance wavelength.

[1] O. Painter, R. Lee, A. Sherer, A. Yariv, J. O'Brien, P. Dapkus, and I. Kim, Science **284**, 1819 (1999).
[2] J. K. Hwang, H. Y. Ryu, D. Song, I. Y. Han, H. W. Song, H. K. Park, Y. H. Lee, and D. H. Jang, Appl. Phys. Lett. **76**, 2982 (2000).
[3] S. Noda, A. Chutinan, and M. Imada, Nature (London) **407**, 6804 (2000).
[4] C. Smith, R. M. de La Rue, M. Rattier, S. Oliver, H. Benisty, C. Weisbuch, T. Krauss, R. Houdre, and U. Oesterle, Appl. Phys. Lett. **78**, 1487 (2001).
[5] T. Yoshie, A. Scherer, H. Chen, D. Huffaker, and D. Deppe, Appl. Phys. Lett. **79**, 114 (2001).
[6] S. G. Johnson, S. Fan, A. Mekis, and J. Joannopoulos, Appl. Phys. Lett. **78**, 3388 (2001).
[7] E. Miyai and K. Sakoda, Opt. Lett. **26**, 740 (2001).
[8] P. Villeneuve, S. Fan, S. Johnson, and J. Joannopoulos, IEE Proc.: Optoelectron. **145**, 384 (1998).
[9] C. Grillet, O. Pottier, X. Letartre, C. Seassal, P. Rojo-Romeo, P. Viktorovitch, M. L. V. dYerville, and D. Cassagne, Eur. Phys. J.: Appl. Phys. **16**, 37 (2001).
[10] J. Vuckovic, M. Loncar, H. Mabushi, and A. Scherer, Phys. Rev. E **65**, 016 608 (2002).
[11] S. Y. Lin, E. Chow, S. G. Johnson, and J. Joannopoulos, Opt. Lett. **26**, 1903 (2001).
[12] S. G. Johnson, S. Fan, A. Mekis, and J. Joannopoulos, Comput. Sci. Eng. **3**, 38 (2001).
[13] M. Boroditsky, R. Vrijen, T. Krauss, R. Coccioli, R. Bhat, and E. Yablonovitch, J. Lightwave Technol. **17**, 2096 (1999).
[14] W. D. Zhou, J. Sabarinathan, P. Bhattacharya, B. Kochman, E. Berg, P. Yu, and S. Pang, IEEE J. Quantum Electron. **37**, 1153 (2001).
[15] C. Smith, S. Murad, T. Krauss, R. D. L. Rue, and C. Wilkinson, J. Vac. Sci. Technol. B **17**, 113 (1999).
[16] T. Krauss, R. D. L. Rue, and S. Brand, Nature (London) **383**, 699 (1996).
[17] C. Cheng, A. Scherer, R. Tyan, Y. Fainman, G. Witzgall, and E. Yablonovitch, J. Vac. Sci. Technol. B **15**, 2764 (1997).
[18] A. Scherer, O. Painter, B. D'Urso, R. Lee, and A. Yariv, J. Vac. Sci. Technol. B **16**, 3906 (1998).
[19] H. Mossallaei, Ph.D. Dissertation Thesis, University of California, Los Angeles, CA, 2001.
[20] H. Haus, *Waves and Fields in Optoelectronics* (Prentice-Hall, Englewood Cliffs, NJ, 1984).
[21] Y. Takeda, A. Sasaki, Y. Imamura, and T. Takagi, J. Appl. Phys. **47**, 5405 (1976).